ADVANCED ENERGY MATERIALS

Supporting Information

for *Adv. Energy Mater.,* DOI: 10.1002/aenm.202003417

Unraveling the Li Penetration Mechanism in Polycrystalline Solid Electrolytes

Karnpiwat Tantratian, Hanghang Yan, Kevin Ellwood, Elisa T. Harrison, and Lei Chen**

SUPPORTING INFORMATION

Unraveling the Li Penetration Mechanism in Polycrystalline Solid Electrolytes

Karnpiwat Tantratian[1], Hanghang Yan[1,3], Kevin Ellwood[2], Elisa T. Harrison[2,], Lei Chen[1,]**

[1]Department of Mechanical Engineering, University of Michigan-Dearborn, Dearborn, Michigan 48128-1491, United States.

[2]Research and Innovation Center, Ford Motor Company, Dearborn, Michigan 48121, United States.

[3]State Key Laboratory of Advanced Design and Manufacturing for Vehicle Body, Hunan University, Changsha 410082, PR China.

*Corresponding author: Lei Chen E-mail: leichn@umich.edu

Elisa T. Harrison E-mail: eharr188@ford.com

Additional simulation results on the impact of applied current density and stack pressure

(i) Impact of applied current density

The current density majorly determines the Li deposition rate. Under a high applied current density of 1.6 mA cm^{-2}, the deposition thickness reaches 30 µm within 400 s with a fully-developed Li penetrant in the GB as illustrated in **Figure S1**a. On the other hand, a low current density of 0.9 mA cm^{-2} leads to a slower rate and a more uniform Li deposition. Figure S1b shows under the high applied current density, the current density at the Li/GB interface is twice of that at the Li/grain interface. In contrast, under the low applied current density, the current density is more uniform throughout the Li/SE interface.

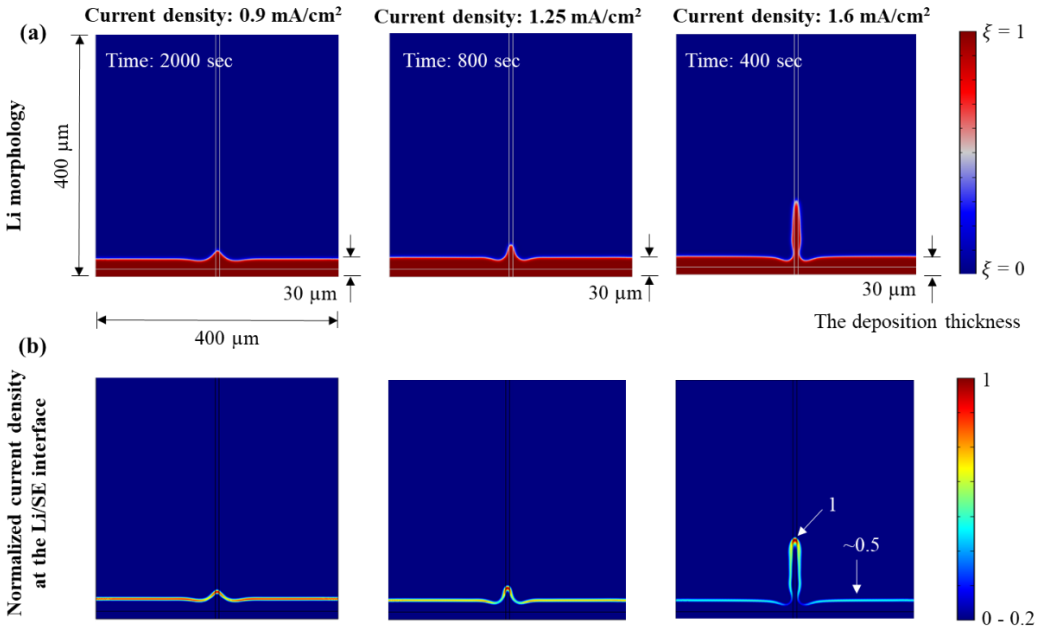

Figure S1. (a) Li morphologies under different applied current density captured when the Li deposition thickness reaches 30 µm. (b) The corresponding current density at the Li/SE interface normalized respected to the maximum current density.

(ii) Impact of stack pressure

Figure S2a demonstrates that although the overall Li deposition is reduced under the high stack pressure, the Li penetrant exists in the GB region. Stack pressure essentially adds compressive stress throughout the domain, including the Li/SE interface where the reaction occurs. Thus, the electrodeposition rate is slowed down. However, the magnitude of stress at the Li/GB and Li/grain interfaces is still largely different due to the inhomogeneous mechanical properties as shown in Figure S2b. Therefore, Li preferentially grows in the GB region where compressive stress at the interface is much smaller.

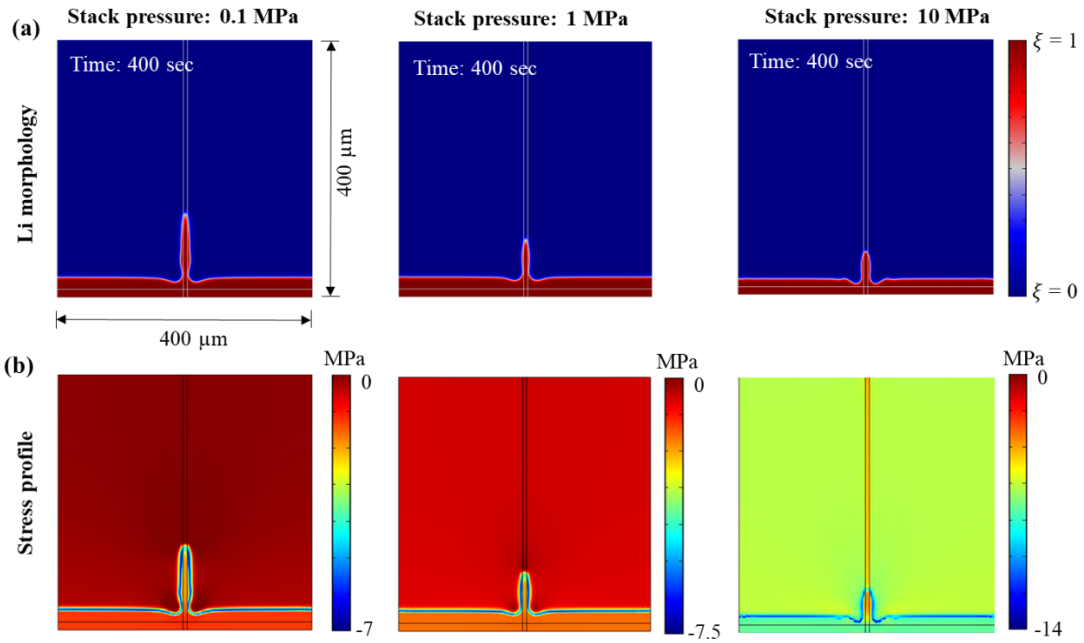

Figure S2. (a) Li morphologies under different stack pressure captured at 400 s. (b) The corresponding stress profile.

The derivation of modified Butler-Volmer equation

At the interface of the Li metal/SE, the electrodeposition process, $Li^+ + e \leftrightharpoons Li$, involves the competing influences of forward and backward reactions. When the forward reaction is dominant, the electrodeposition occurs. In contrast, if the backward reaction is more favorable, the Li metal is dissolved. The net of reaction kinetics can be written in the form of

$$R_t = -k_0 \left\{ \exp\left[\frac{-(\mu_t^{ex} - \mu_1)}{RT}\right] - \exp\left[\frac{-(\mu_t^{ex} - \mu_2)}{RT}\right] \right\}, \quad \text{(S1)}$$

where k_0 is the reaction rate constant. μ_t^{ex} is the excess potential at the transition state. μ_1 and μ_2 are the electrochemical potential at the states of Li metal and Li-ion, respectively. To derive the expression for μ_1 and μ_2, it is convenient to write the potential for each component in the reaction,

$$\overline{\mu_{Li}} = RTlna_{Li} + \mu_{Li}^0 + Pv_{Li}, \quad \text{(S2)}$$

$$\overline{\mu_+} = RTlna_+ + \mu_+^0 + F\emptyset_s, \quad \text{(S3)}$$

$$\overline{\mu_-} = RTlna_- + \mu_-^0 - F\emptyset_e, \quad \text{(S4)}$$

where $\emptyset_s$ and $\emptyset_e$ are the electrostatic potential in the SE and Li metal electrode, respectively. Pv_{Li} refers to the mechanical contribution that shifts the electrochemical potential of the electrode, where P is the hydrostatic pressure acting on the reaction front and v_{Li} is the molar volume of Li metal. μ_1 and μ_2 can be expressed as follows:

$$\mu_1 = \overline{\mu_+} + n\overline{\mu_-} = RTlna_+a_- + \mu_+^0 + \mu_-^0 - F(\Delta\emptyset), \quad \text{(S5)}$$

$$\mu_2 = \overline{\mu_{Li}} = RTlna_{Li} + \mu_{Li}^0 + Pv_{Li}, \quad \text{(S6)}$$

where $\Delta\emptyset = \emptyset_e - \emptyset_s$ represents the electric potential difference at the Li/SE interface. Next, to define μ_T^{ex}, we assume that the electrostatic potential varies linearly across the Li/SE interface. In addition, due to the nature of a solid-state system, the mechanical stress is intensified at the contact areas of the Li/SE interface where the reaction takes place. Thus, we assume that the mechanical action also contributes to the excess energy of the transition state, described as

$$\mu_T^{ex} = RTln\gamma_T + \alpha_a(F\emptyset_s - F\emptyset_e + \mu_+^0 + \mu_-^0) + \alpha_c(\mu_M^0) + Pv_{Li}, \quad \text{(S7)}$$

where γ_T is the non-ideal activity coefficient of the transition state. The anodic and cathodic charge transfer coefficients yield $\alpha_a = 1 - \alpha$ and $\alpha_c = \alpha$, respectively, where α is an asymmetric factor varying from 0 to 1.

The equilibrium state is reached when $\Delta\mu = \mu_1 - \mu_2 = 0$, or

$$\Delta\mu = \frac{RT}{F} ln\frac{a_+a_-}{a_{Li}} + E^o - \Delta\emptyset^{eq} - \frac{Pv_{Li}}{F} = 0. \quad \text{(S8)}$$

Thus, we have the equilibrium potential of the reaction under the excess pressure, P, expressed as

$$\Delta\emptyset^{eq} = \left(E^o - \frac{Pv_{m,Li}}{F}\right) + \frac{RT}{F} ln\frac{a_+a_-}{a_{Li}}, \quad \text{(S9)}$$

where

$$E^o = \frac{\mu_+^0 + \mu_-^0 - \mu_{Li}^0}{F} \quad \text{(S10)}$$

is the standard potential difference between the reactants and products. Without the pressure acting on the interface (P = 0), Equation S9 yields the classical Nernst equation. On the contrary, the presence of the mechanical action at the Li/SE interface shifts the standard potential

difference E^o, resulting in a new equilibrium potential and thus a new exchange reaction rate or current density. In addition, the sign of *P*, is dependent on the state of stress at the interface: $P > 0$ refers to compression and $P < 0$ refers to tension. When the system is out of equilibrium, $\Delta\mu \neq 0$, the electrochemical reaction rate is regulated by the overpotential, which is defined as

$$\eta = \Delta\emptyset - \Delta\emptyset^{eq} = \Delta\emptyset - E^o - \frac{RT}{F} ln \frac{a_+ a_-}{a_{Li}} + \frac{P v_{Li}}{F}. \tag{S11}$$

The total overpotential (η) is comprised of (i) the activation overpotential, $\eta_a = \Delta\emptyset - E^o$, (ii) concentration overpotential, $\eta_c = -\frac{RT}{F} ln \frac{a_+ a_-}{a_{Li}}$, and (iii) the change of total overpotential due to the mechanical action or the mechanical overpotential, $\eta_m = \frac{P v_{Li}}{F}$. By plugging in Equations S5-S7 into Equation S1, the net reaction rate is expressed as

$$R_t = -k_0 \left\{ \exp\left[\frac{RT ln \frac{a_{Li}}{\gamma_T} + (1-\alpha) F (\Delta\emptyset - E^o)}{RT} \right] - exp\left[\frac{RT ln \frac{a_+ a_-}{\gamma_T} - \alpha F (\Delta\emptyset - E^o) - P v_{Li}}{RT} \right] \right\}. \tag{S12}$$

We assume that $a_+ = c_+$ and $a_- = c_-$, where c_+ and c_- are the normalized concentrations of Li-ion and electrons, respectively. With the definition of the overpotential in Equation S11, Equation S12 can be written in the form of

$$R_t = -R_{00} \left\{ \exp\left[\frac{(1-\alpha) F (\eta_a + \eta_c)}{RT} \right] - \exp\left[\frac{-\alpha F (\eta_a + \eta_c) - F\eta_m}{RT} \right] \right\}, \tag{S13}$$

or

$$I = -I_{00}\left\{\exp\left[\frac{(1-\alpha)F(\eta_a+\eta_c)}{RT}\right] - \exp\left[\frac{-\alpha F(\eta_a+\eta_c)-F\eta_m}{RT}\right]\right\}, \quad \text{(S14)}$$

where $R_{00} = k_0(c_+c_-)^{1-\alpha}{a_{Li}}^{\alpha}{\gamma_T}^{-1}$ and $I_{00} = ek_0(c_+c_-)^{1-\alpha}{a_{Li}}^{\alpha}{\gamma_T}^{-1}$ are the exchange reaction rate and current density, respectively. By assuming that the electrons are abundant on the Li metal surface (c_- = 1), a_{Li} = 1, and plugging in $\eta_c = -\frac{RT}{F}ln\frac{c_+c_-}{a_{Li}}$, Equation S14 can be rearranged as,

$$I = -I_0\left\{\exp\left[\frac{(1-\alpha)F\eta_a}{RT}\right] - c_+\exp\left[\frac{-\alpha F\eta_a - F\eta_m}{RT}\right]\right\}, \quad \text{(S15)}$$

where $I_0 = I_{00}\left(\frac{c_+}{a_{Li}}\right)^{-(1-\alpha)}$ or $I_0 = ek_0a_{Li}{\gamma_T}^{-1}$. If $\eta_a < 0$, the anodic reaction rate is smaller than the rate of cathodic reaction; thus, the reduction of the electrolyte takes place ($I > 0$). On the other hand, if ($\eta_a > 0$), the anodic reaction rate is more favorable, leading to the dissolution process of Li metal ($I < 0$). In the case of the electrodeposition ($\eta_a < 0$) under the presence of the compressive stress ($\eta_m > 0$), the cathodic reaction rate is reduced due to the mechanical overpotential, retarding the electrodeposition process.

Moreover, Equation S16 can be rearranged as

$$I = -I_0 exp\left[\frac{-(1-\alpha)F\eta_m}{RT}\right]\left\{exp\left[\frac{(1-\alpha)F\eta}{RT}\right] - c_+ exp\left[\frac{-\alpha F\eta}{RT}\right]\right\}, \quad \text{(S16)}$$

where η is the overpotential across the deformed surface $\eta = \eta_a + \eta_m$. Therefore, alternatively, it can be thought that the surface stress impacts the magnitude of the exchange current density, $I_0^* = I_0\exp\left[\frac{-(1-\alpha)F\eta_m}{RT}\right]$. Specifically, if the interfacial stress is compressive, $\eta_m > 0$, the exchange current density is diminished, resulting in the reduced reaction rate.

Note that the formulation of our modified Butler-Volmer equation is different from the one proposed by Monroe and Newman,[1] which implies that the mechanical action shifts the rate of anodic reaction. Nevertheless, the impact of the mechanical stress at the reaction interface from both formulations are the same: compressive stress diminishes the electrodeposition rate, while it is the opposite for the tensile stress.

Electro-chemo-mechanical phase-field equation

In this phase-field model, the order parameter, ξ, is introduced to describe the phase evolution of Li metal: $\xi = 1$ refers to the Li metal, and $\xi = 0$ refers to the SE. The phase transformation rate is driven by the electrodeposition rate of Li, expressed as $\frac{\partial \xi}{\partial t} = R_t$. Recall Equation S13 for the expression of the modified reaction kinetics. As the system is far from equilibrium, the driving force due to the concentration overpotential (η_c) is relatively small compared with the driving force due to the activation potential (η_a). Due to the solid nature of the system, the driving force from the change of overpotential due to the mechanical action (η_m) is significant. Therefore, we assume that the evolution of the phase-field linearly changes with the concentration overpotential, while varies exponentially with the activation and mechanical overpotentials.[2] The phase field equation is described as

$$\frac{\partial \xi}{\partial t} = -L_0(g'(\xi) - k\nabla^2\xi) - L_\eta h'(\xi)\left\{\exp\frac{(1-\alpha)F\eta_a}{RT} - c_+\exp\left[\frac{-\alpha F\eta_a - F\eta_m}{RT}\right]\right\} + \delta_N, \quad \text{(S17)}$$

where L_0 and L_η are the coefficients related to the interfacial energy and reaction, respectively. $h(\xi) = \xi^3(10 - 15\xi + 6\xi^2)$ is an interpolation function applied to describe the reaction at the diffuse interface. $g(\xi) = W\xi^2(1-\xi)^2$ is an arbitrary double well function, where W is the barrier height. k is a gradient coefficient. The driving force of dendrite nucleation, δ_N, represents the driving of Li dendrite due to the trapped electrons in SE. See the next section for the complete details of the nucleation model.

In addition, as the SE contains microstructural structures such as grain boundary, to differentiate grain boundary from the bulk grain (GB) in the SE phase, we introduce another non-conservable phase field parameter, φ, which is unity in the grain boundary and zero in the bulk. By scaling with this phase field parameter (φ), the properties of the SE, for example, elastic modulus and

Li-ion diffusion coefficients, smoothly changes from the properties of bulk grain to that of GB at the interface. The equation can be written as,

$$\frac{\partial \varphi}{\partial t} = -{L_0}^s \frac{\partial F}{\partial \varphi}, \quad \text{(S18)}$$

where ${L_0}^s$ is the interfacial mobility of the phase in SE. The phase-field equations, Equation S15 and S16, are solved together with the mass transport, electrostatic distribution, and stress equilibrium equations. The diffusion of Li-ion is governed by the classical Nernst-Plank equation, expressed as

$$\frac{\partial c_+}{\partial t} = \nabla \cdot \left[D^{eff} \nabla c_+ + \frac{D^{eff} \nabla c_+}{RT} nF \nabla \phi \right] - \frac{c_s}{c_0} \frac{\partial \xi}{\partial t}, \quad \text{S19)}$$

where $D^{eff} = h(\xi) D_{Li} + (1 - h(\xi))(h(\varphi) D_{GB} + (1 - h(\varphi)) D_G)$ is the effective diffusion coefficient. D_{Li}, D_{GB} and D_G are diffusion coefficients of Li-ion in Li metal, GB, and grain of SE, respectively. The last term on the right-hand side of Equation S17 relates to a sink term representing the decrease of Li-ions in the SE due to the electrodeposition process. c_s = 7.64×10^4 mol m^{-3} is the site density of Li metal, and c_0 is the bulk concentration. The electrostatic potential is governed by the Poisson's equation with a source term representing the charges annihilation at the reaction interface, expressed as

$$\nabla \cdot \left[\sigma^{eff} \nabla \phi \right] = I_R, \quad \text{S20)}$$

where $\sigma^{eff} = h(\xi) \sigma_{Li} + (1 - h(\xi))(h(\varphi) \sigma_{GB} + (1 - h(\varphi)) \sigma_G)$ is the effective conductivity. The source term, $I_R = nF c_+ \partial \xi / \partial t$, is non-zero at the metal/electrolyte interface where $\partial \xi / \partial t > 0$. The complete details of the model development can be found in reference.[2]

Mechanical stress is generated due to the volume change of the Li metal anode during Li deposition. The contact surface, microstructural features and creep behavior of Li metal are the factors for internal stress evolution. However, for simplicity, in this work, (i) the contact mechanics is not considered, and (ii) the inelastic strain due to the volume expansion of Li metal is the only source of the internal stress evolution. The stress equilibrium is solved to get the Li stress distributions at the interface, which is expressed as,

$$\nabla \cdot \boldsymbol{\sigma} = 0 \tag{S21}$$

where

$$\boldsymbol{\sigma} = \boldsymbol{C^{eff}} \cdot \boldsymbol{\varepsilon^{el}} = \boldsymbol{C^{eff}} \cdot \left(\boldsymbol{\varepsilon} - \boldsymbol{\varepsilon^{0}}\right). \tag{S22}$$

$\boldsymbol{C^{eff}}(\xi) = h(\xi)\boldsymbol{C}_{Li} + (1 - h(\xi))(h(\varphi)\boldsymbol{C}_{GB} + (1 - h(\varphi))\boldsymbol{C}_{G})$ is the effective elastic stiffness tensor. ε^{el} is the elastic strain, and small deformation theory is assumed. ε^{0} is an inelastic strain due to the volume expansion of Li metal during the Li deposition process. It can be expressed as $\boldsymbol{\varepsilon^{0}} = \boldsymbol{K_{ii}}\xi$, where $\boldsymbol{K_{ii}}$ is a constant diagonal matrix. Nonetheless, $\boldsymbol{K_{ii}}$ is unknown; thus, to obtain the value for $\boldsymbol{K_{ii}}$, the calibration process is required.

The magnitude of the Li interfacial stress is likely to be in an order of a few megapascal due to the very low yield strength of Li and its creep flow behavior. However, according to the formulation of mechanical overpotential, $\eta_m = Pv_{Li}/\,F$, a few megapascal of stress at the interface (P = 1 - 10 MPa) leads to a small mechanical overpotential, $\eta_m = Pv_{m,Li}/F \approx 10^{-4} - 10^{-3}\,V$, which would exert no influence on the reaction rate, particularly when $|\eta_a| \gg |\eta_m|$. However, due to the nature of electrochemical reaction in a solid system, the mechanical stress

should play a critical role in governing the Li deposition rate.[3] Therefore, we introduce a constant, *C*, to correct the change of the overpotential due to the mechanical action. The mechanical overpotential is now expressed as

$$\eta_m = C\frac{Pv_{m,Li}}{F}. \quad \text{(S23)}$$

For electrodeposition ($\eta_a < 0$), the cathodic reaction rate should remain quite larger than the anodic reaction rate. Thus, the exponent term for the cathodic reaction rate (Equation S15) should remain positive: $-\alpha F\eta_a - F\eta_m > 0$ or $-\alpha\eta_a > \eta_m$. In this work, we assume α = 0.5; therefore, the mechanical overpotential should be less than the half of the activation overpotential $-\eta_a/2 > \eta_m$. Thus, the range of *C* is defined as $0 < C < F\eta_a/2Pv_{m,Li}$.

Li dendrites nucleation model

Following the work of Tian et al.[4], the driving force of dendrite nucleation, δ_N, is given by

$$\delta_N = \begin{cases} 1, & P_N = 1 - \exp(-J\Delta t) > \text{random}\,[0,1] \\ 0, & \text{otherwise} \end{cases}, \tag{S24}$$

where P_N is a nucleation probability described by a Poisson distribution. J is the Li nucleation rate, which is expressed as

$$J = J_0 \exp\left(-\frac{\sigma_{inhomo}\Delta G}{k_b T}\right), \tag{S25}$$

where J_0 is a constant related to the nucleation rate. σ_{inhomo} is a correction factor for heterogeneous nucleation. ΔG is the activation energy, which is a function of the chemical potential difference, written in the form of

$$\Delta G = \frac{16\pi\gamma^3 {v_{Li}}^2}{3\Delta\mu^2}, \tag{S26}$$

where γ is the interfacial energy between the Li precipitates and the SE. v_{Li} is the molar volume of Li metal. The chemical potential difference is the summation of concentration and activation overpotential, expressed as

$$\Delta\mu = F\eta = F(\eta_a + \eta_c) = F(\Delta\emptyset - E^o) - RTln\frac{c_+ c_-}{a_{Li}}, \tag{S27}$$

where c_- is the normalized electron concentration and defined as c_- = 1 + $\breve{c_e}$. $\breve{c_e}$ is the (normalized) trapped excess electron concentration. The activity of Li metal, a_{Li}, is unity and in the bulk SE the normalized concentration of Li-ion, c_+ is unity as well. In the scenario that the

trapped electrons concentration $\breve{c}_e > 0$, the concentration overpotential is rising, and thus, increasing the driving force for Li nucleation. More details can found in reference.[4]

Change in chemical potential due to the mechanical stress

The effect of mechanical stress on the chemical is derived from the classical Gibbs-Duhem Equation,

$$Nd\mu = VdP - SdT, \tag{S28}$$

where μ is the chemical potential, N is the mole of substance, S is entropy, V is volume, P is hydrostatic pressure, and T is temperature. For solids, the following assumptions are made: (i) N = 1, (ii) the stress is uniform over the molar volume, V_m, (iii) the metal behaves linearly elastic, and (iv) the process is isothermal (dT = 0).[5] Due to the low compressibility of the solids, the volume V can be described as $V = V_m \exp(-\frac{P}{K})$,[6] where K is the bulk modulus. By integrating pressure from the initial to the final state, the equation is expressed as

$$\Delta\mu = \int_{P_1}^{P_2} V(P)dP = \int_{P_1}^{P_2} V_m \exp\left(-\frac{P}{K}\right) dP \approx V_m\Delta P - \frac{\Delta P^2 V_m}{2K}. \tag{S29}$$

$V_m\Delta P$ represents the stress energy, and $\Delta P^2 V_m/2K$ is associated with the strain energy. As K is large; therefore, the contribution from the strain energy can be negligible. Consequently, the change of chemical potential due to the mechanics is reduced to

$$\Delta\mu = V_m\Delta P. \tag{S30}$$

Calibration and verification of eigenstrain due to the volume expansion

In this work, we simplify the complicated mechanics problems by assuming that volume expansion of Li metal is solely the origin of the internal stress generation and the contact problem is not considered. The values of eigenstrain should give a similar magnitude of interfacial compressive stress to those obtained from analytical or computational approaches, which fully account for the mechanics problems. X. Zhang et al.[7] performed contact stress calculations by involving deformation, creep, and the volume change of Li metal during the Li depositing/stripping process. The result indicates the maximum contact stress at the Li/SE interface is approximately -5.5 ± 1.1 MPa. In addition, Q. Tu et al.[8] carried out a theoretical study on the impact of the surface irregularity on Li deposition behavior by considering interfacial contact of Li/SE and plastic behavior of Li. The results show the maximum stress could reach -5.8 MPa around the defects (as plotted in Figure 1e). Both studies inform a magnitude of stress at the Li/SE interface is around a few megapascals (≤ 7 MPa). So, we determined $\boldsymbol{K_{ii}}$ values by changing the value of eigenstrain until the magnitude of stress at the Li/SE interface generally agrees with those analytical approaches.

Simulation details for Li deposition in a solid electrolyte (SE) with a single GB

The simulation is carried out in COMSOL Multiphysics 5.4, employing the finite element analysis. The model involves 5 governing equations, Equation S15-S19, which govern the phase fields order parameters (ξ, φ), Li-ion concentration (c), the electric field ($\emptyset$), and stress-strain relation, respectively. **Figure S3** illustrates the geometry and initial and boundary condition for all equations. The applied current density of 1.6 mA cm^{-2} can be correlated to the applied electric potential of 62.5 mV through Ohm's law: $J = \sigma \Delta \emptyset / L$, where L is the length of the electrolyte domain. We set the initial electric potential in the SE is 62.5 mV, while the initial electric potential in the electrode is 0 mV. The initial normalized Li-ion concentration in the SE and the electrode domain are 1 and 0, respectively. The initial stress and displacement in both SE and electrode domains are zero. The Dirichlet boundary conditions are applied at the opposite side of the electrode with the normalized Li-ion concentration of 1 and the electric potential of 62.5 mV. In mechanics part, the roller boundaries are applied at the top and bottom. The right boundary is fixed, and the left boundary is subjected to either fixed displacement or stack pressure. Through calibration, the values of K_{11}, K_{22}, and K_{33} were determined to be $2.1\ x\ 10^{-4}$. The others model parameters are listed in Table S1.

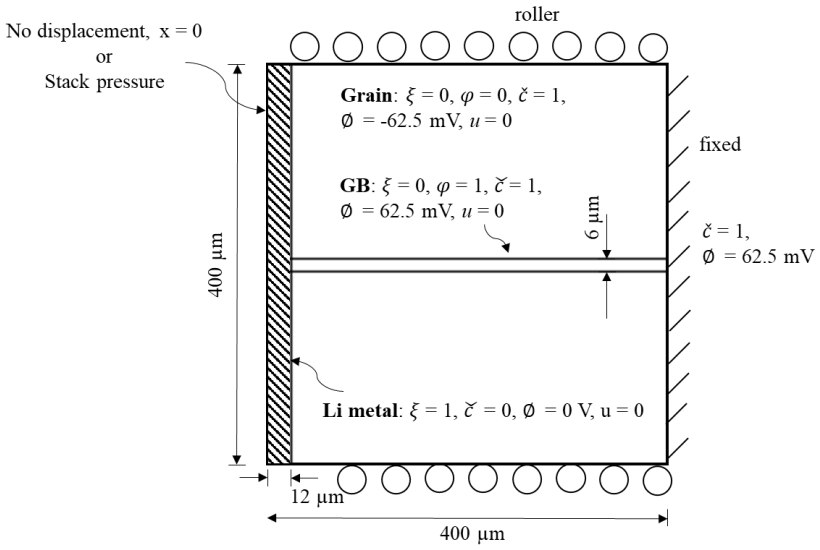

Figure S3. The geometry and initial and boundary condition of the Li deposition simulation in SE containing a single GB.

Table S1. Model parameters in simulation of Li deposition in a solid electrolyte (SE) with a single grain boundary. The characteristic values used in normalization are the following: l_0 = 100 x 10^{-6} m, Δt_0 = 4000 s, ΔE_0 = 5 x 10^5 J m^{-1}, c_s = 7.64 x 10^4 mol m^{-3}.

	Unit	Real Value			Normalization	Normalized Value		
		Li	SE	GB		Li	SE	GB
System Size (l)	μm	400 x 400			$\breve{l} = l/l_0$	4 x 4		
Time step (Δt)	s	0.2			$\breve{\Delta t} = \Delta t/\Delta t_0$	5 x 10^{-5}		
Li-ion diffusion coefficient (D)	m^2 s^{-1}	5.5 x 10^{-15}	5.5 x 10^{-12}	5.5 x 10^{-12}	$\breve{D} = D/({l_0}^2/\Delta t_0)$	2.2 x 10^{-3}	2.2	2.2
Conductivity (σ)	S m^{-1}	1 x 10^7	0.1	0.1	$\breve{\sigma} = \sigma(RT\Delta t_0)/(c_0{l_0}^2F^2)$	1.0 x 10^9	10	10
Elastic Modulus (E)	Pa	5.0 x 10^9	50 x 10^9	100 x 10^9	-	-	-	-
Poisson ratio	-	0.3	0.25	0.25	-	0.3	0.25	0.25
Gradient energy coefficient (κ)	J/m	3 x 10^{-5}	-	-	$\breve{\kappa} = \kappa\ /\ (E_0{l_0}^2)$	6.0 x 10^{-3}	-	-
Interfacial mobility (L_σ)	m^3 $(Js)^{-1}$	2.5 x 10^{-6}	0	0	$\breve{L_\sigma} = L_\sigma E_0 \Delta t_0$	5.0 x 10^3	0	0
Reaction constant (L_η)	s^{-1}	15.625	-	-	$\breve{L_\eta} = L_\eta \Delta t_0$	6.25x 10^4	-	-
Symmetric factor (α)	-	0.5	-	-	-	0.5	-	-
Stress correction term(C)	-	12.5	-	-	-	12.5	-	-
Molar volume ($v_{m,Li}$)	m^3 mol^{-1}	1.3 x 10^{-5}	-	-	-	-	-	

Simulation of Li deposition in a polycrystalline LLZO

The simulations are performed in COMSOL Multiphysics 5.4, which based on finite element method. The tetrahedral mesh is applied and is fined enough in the GB region such that the calculations are run smoothly. The model involves 5 the governing equations, Equation S15-19. **Figure S4** shows the geometry and all initial and boundary conditions. The domain sized was 61.25 x 35 μm. The grain structure is randomly generated with the approximate grain size of 7.5 μm. The thickness of the GB and initial Li metal electrode is 0.5 and 1.5 μm, respectively. The current density of 2.0 mA cm^{-2} is applied (correlated to the overpotential of 62.5 mV). The initial and boundary condition details are similar to the previous section. However, the calculated and measured LLZO properties such as ionic conductivity and mechanical property and a new set of parameters are utilized (**Table S2**). The elastic modulus of the grain is 158 GPa, while the elastic modulus of the softening GB is approximately 92 GPa.[9] The trapped electrons concentration of 0.337 mol/L[4,10] is applied throughout the GB domain. The inelastic strain to the volume expansion, the matrix $\boldsymbol{K_{ii}}$, are $K_{11} = K_{22} = 5\ x\ 10^{-5}$ and $K_{33} = 2x\ 10^{-4}$.

The factor *C* is approximated through the calibration. Here, LLZO properties are utilized. Under such a high current density of 2.0 mA cm^{-2}, the Li dendrite penetration is expected. The *C* factor is adjusted, such that the resulting Li morphology in LLZO resembles with the existing experimental observation that shows Li dendrites along the GB.[11] Thus, C = 24 is obtained.

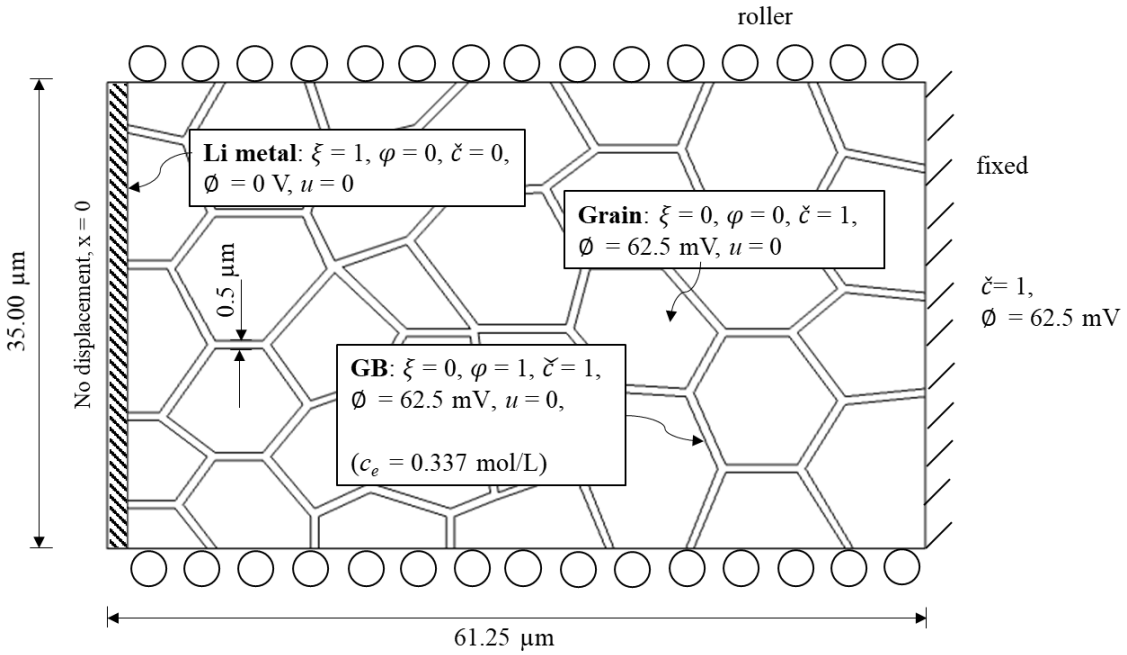

Figure S4. The geometry and initial and boundary condition of the Li deposition simulation in polycrystalline LLZO.

Table S2. Model parameters in simulation of Li deposition in LLZO. The characteristic values used in normalization are the following: l_0 = 35 x 10^{-6} m, Δt_0 = 10000 s, ΔE_0 = 5 x 10^5 J m^{-1}, c_s = 7.64 x 10^4 mol m^{-3}.

	Unit	Real Value			Normalization	Normalized Value		
		Li	LLZO	GB		Li	LLZO	GB
System Size (l)	μm	61.25 x 35			$\check{l} = l/l_0$	1.75 x 1.0		
Time step (Δt)	s	10			$\check{\Delta t} = \Delta t/\Delta t_0$	1 x 10^{-4}		
Li-ion diffusion coefficient (D)	m^2 s^{-1}	1 x 10^{-16}	1 x 10^{-13}	1 x 10^{-13}	$\check{D} = D/({l_0}^2/\Delta t_0)$	8.2 x 10^{-4}	8.2 x 10^{-1}	8.2 x 10^{-1}
Conductivity (σ)	S m^{-1}	2 x 10^7	2 x 10^{-2}	2 x 10^{-2}	$\check{\sigma} = \sigma(RT\Delta t_0)/(c_0{l_0}^2F^2)$	10 x 10^9	10	10
Elastic Modulus (E)	Pa	5 x 10^9	92 x 10^9	158 x 10^9	-	-	-	-
Poisson ratio	-	0.3	0.25	0.25	-	0.3	0.25	0.25
Gradient energy coefficient (κ)	J/m	1.1 x 10^{-6}	-	-	$\check{\kappa} = \kappa / (E_0{l_0}^2)$	1.8 x 10^{-3}	-	-
Interfacial mobility (L_σ, L_σ^s)	m^3 $(Js)^{-1}$	4.4 x 10^{-6}	0	0	$\check{L_\sigma} = L_\sigma E_0 \Delta t_0$	2.2 x 10^4	0	0
Reaction constant (L_η)	s^{-1}	27.5	-	-	$\check{L_\eta} = L_\eta \Delta t_0$	2.75x 10^5	-	-
Symmetric factor (α)	-	0.5	-	-	-	0.5	-	-
Stress correction term(C)	-	24	-	-	-	24	-	-
Molar volume ($v_{m,Li}$)	m^3 mol^{-1}	1.3 x 10^{-5}	-	-	-	-	-	
Bulk Li-ion concentration (c_s)	mol m-^{3}	-	42.2 x 10^3	42.2 x 10^3	-	-	-	-
Inelastic strain component K_{11}	-	5 x 10^{-4}	-	-	-	-	-	-
Inelastic strain component K_{22}	-	5 x 10^{-4}	-	-	-	-	-	-
Inelastic strain component K_{33}	-	2 x 10^{-3}	-	-	-	-	-	-
Nucleation parameters								
Nucleation rate pre-factor (J_0)	-	800	-	-	-	-	-	-
correction factor (σ_{inhomo})	-	1	-	-	-	-	-	-
Excess electron concentration (c_e)	mol m^{-3}	-	0	337	$\check{c_e} = c_e/c_{e0}$	-	0	0.337
Interfacial energy (γ)	J m^{-2}	0.05	-	-	-	-	-	-

References

[1] C. Monroe, J. Newman, *J. Electrochem. Soc.* **2005**, *152*, A396.

[2] L. Chen, H. W. Zhang, L. Y. Liang, Z. Liu, Y. Qi, P. Lu, J. Chen, L. Q. Chen, *J. Power Sources* **2015**, *300*, 376.

[3] P. Wang, W. Qu, W. L. Song, H. Chen, R. Chen, D. Fang, *Adv. Funct. Mater.* **2019**, *29*, 1.

[4] H. K. Tian, Z. Liu, Y. Ji, L. Q. Chen, Y. Qi, *Chem. Mater.* **2019**, *31*, 7351.

[5] S. Sarkar, W. Aquino, *Electrochim. Acta* **2013**, *111*, 814.

[6] H. Ma, X. Xiong, P. Gao, X. Li, Y. Yan, A. A. Volinsky, Y. Su, *Sci. Rep.* **2016**, *6*, 1.

[7] X. Zhang, Q. J. Wang, K. L. Harrison, S. A. Roberts, S. J. Harris, *Cell Reports Phys. Sci.* **2020**, *1*, 100012.

[8] Q. Tu, L. Barroso-Luque, T. Shi, G. Ceder, *Cell Reports Phys. Sci.* **2020**, *1*, 100106.

[9] S. Yu, D. J. Siegel, *ACS Appl. Mater. Interfaces* **2018**, *10*, 38151.

[10] H. K. Tian, B. Xu, Y. Qi, *J. Power Sources* **2018**, *392*, 79.

[11] E. J. Cheng, A. Sharafi, J. Sakamoto, *Electrochim. Acta* **2017**, *223*, 85.